Applied Physics Letters

Engineering room-temperature multiferroicity in Bi and Fe codoped $BaTiO_3$

Cite as: Appl. Phys. Lett. **117**, 012901 (2020); https://doi.org/10.1063/5.0004785
Submitted: 14 February 2020 . Accepted: 19 June 2020 . Published Online: 06 July 2020

Pratap Pal, Tapas Paramanik, Krishna Rudrapal, Supriyo Majumder, Satish Yadav, Sudipta Mahana, Dinesh Topwal, Ram Janay Choudhary, Kiran Singh, Ayan Roy Chaudhuri, and Debraj Choudhury

Applied Physics Letters ARTICLE scitation.org/journal/apl

Engineering room-temperature multiferroicity in Bi and Fe codoped $BaTiO_3$

Cite as: Appl. Phys. Lett. **117**, 012901 (2020); doi: 10.1063/5.0004785
Submitted: 14 February 2020 · Accepted: 19 June 2020 ·
Published Online: 6 July 2020

Pratap Pal,[1] Tapas Paramanik,[1,2] Krishna Rudrapal,[3] Supriyo Majumder,[4] Satish Yadav,[4] Sudipta Mahana,[5] Dinesh Topwal,[6,7] Ram Janay Choudhary,[4] Kiran Singh,[4,8] Ayan Roy Chaudhuri,[3,9] and Debraj Choudhury[1,a)]

AFFILIATIONS

[1]Department of Physics, Indian Institute of Technology Kharagpur, West Bengal 721302, India
[2]Department of Physics, School of Sciences, National Institute of Technology Andhra Pradesh, Tadepalligudem 534101, India
[3]Advanced Technology Development Centre, Indian Institute of Technology Kharagpur, West Bengal 721302, India
[4]UGC-DAE Consortium for Scientific Research, University Campus, Khandwa Road, Indore 452001, India
[5]Rajdhani College, Baramunda square, Bhubaneswar 751003, India
[6]Institute of Physics, Sachivalaya Marg, Bhubaneswar 751005, India
[7]Homi Bhabha National Institute, Training School Complex, Anushakti Nagar, Mumbai 400085, India
[8]Dr. B. R. Ambedkar National Institute of Technology, Jalandhar 144011, India
[9]Materials Science Centre, Indian Institute of Technology Kharagpur, West Bengal 721302, India

[a)]Author to whom correspondence should be addressed: debraj@phy.iitkgp.ac.in

ABSTRACT

Fe doping into $BaTiO_3$ stabilizes the paraelectric hexagonal phase in place of the ferroelectric tetragonal one. We show that simultaneous doping of Bi along with Fe into $BaTiO_3$ effectively enhances the magnetoelectric (ME) multiferroic response (both ferromagnetism and ferroelectricity) at room temperature, through careful tuning of Fe valency along with the controlled recovery of the ferroelectric-tetragonal phase. We also report a systematic increase in large dielectric constant values as well as reduction in loss tangent values with relatively moderate temperature variation of the dielectric constant around room temperature with increasing Bi doping content in $Ba_{1-x}Bi_xTi_{0.90}Fe_{0.10}O_3$ ($0 \leq x \leq 0.10$), which makes the higher Bi–Fe codoped sample ($x = 0.08$) promising for use as a room-temperature high-κ dielectric material. Interestingly, the $x = 0.08$ (Bi–Fe codoped) sample is not only found to be ferroelectrically (~20 times) and ferromagnetically (~6 times) stronger than $x = 0$ (only Fe-doped) at room temperature, but also observed to be better insulating (larger bandgap) with indirect signatures of larger ME coupling as indicated from anomalous reduction of the magnetic coercive field with decreasing temperature. Thus, room-temperature ME multiferroicity has been engineered in Bi and Fe codoped BTO ($BaTiO_3$) compounds.

Room-temperature magnetoelectric (ME) multiferroic materials are extremely promising for future technological applications.[1,2] In this regard, efforts toward turning $BaTiO_3$ (a strong proper ferroelectric[3]) into a multiferroic material by Fe[4,5] (or other transition metals like Mn,[6] Co,[7] etc.) doping has attracted a lot of attention. However, the observed multiferroicity in Fe-doped BTO is seen to be of mixed phase kind where the ferromagnetism arises from the majority paraelectric-hexagonal phase and weak ferroelectricity due to a minority tetragonal phase.[5] Thus, in such a case, the ME coupling is naturally supposed to be weak due to the independent origin of two ferroic orders at two different structural units. So, the necessity is to stabilize the tetragonal phase, even in this magnetically Fe-doped BTO compound, such that both ferroelectricity and ferromagnetism can emerge from the same tetragonal phase, which may lead to better ME coupling along with pronounced ferroelectricity. It is important to note that for a material to be a potential room-temperature multiferroic, it is desirable to have (a) a strong ferroelectric polarization, (b) a high ferromagnetic remanent moment, and (c) a low leakage-current density (i.e., highly insulating) along with (d) ME coupling between the two ferroic-orders.[8]

With these goals, we examine polycrystalline Ba_{1-x} $Bi_xTi_{0.90}Fe_{0.10}O_3$ compounds ($0 \leq x \leq 0.10$) and show that with increasing Bi doping content not only the paraelectric-hexagonal phase of $x = 0$ (only Fe-doped BTO) gets destabilized (with concomitant recovery of the ferroelectric-tetragonal phase), but also there is a surprising and

significant enhancement of room-temperature ferromagnetism. Interestingly, we find that the observed ferroelectricity is strongest around $x = 0.02$ and ferromagnetism around $x = 0.08$, while the intermediate $x = 0.05$ shows an indirect signature of most robust ME-coupling (see Fig. 1).

All phase pure (related to BTO hexagonal and tetragonal phases only) polycrystalline samples which were prepared via solid state reactions (for details refer to Ref. 5) were characterized using XRD and Raman measurements. Dielectric and magnetic measurements were performed using a Keysight E4980A LCR meter and SQUID-VSM, respectively. Electron Paramagnetic Resonance (EPR) measurements were carried out using a Bruker spectrometer. Intrinsic ferroelectric properties have been investigated using ferroelectric PUND (Positive Up Negative Down) and temperature dependent pyroelectric measurements.[5] XANES (X-ray absorption near edge spectroscopy) and XPS (X-ray photoelectron spectroscopy) measurements were carried out at the P-65 beamline in a PETRA-III synchrotron source, DESY, Hamburg, Germany and using an in-house PHI 5000 Versaprobe-II spectrometer, respectively, while the diffused reflectance spectra were acquired using a Cary 5000 UV-Visible near-infrared spectrophotometer.

Figure 2(a) covers the 2θ range in the XRD spectrum which includes the strongest diffraction peaks from the hexagonal [H(110)] and the tetragonal [T(101)] BTO phases (also see Fig. S1 of the supplementary material). While $x = 0$ crystallizes in the hexagonal phase, with increasing x, the tetragonal phase gets fully recovered as observed from the systematic increase in tetragonal T(101) peak intensity and concomitant decrease in hexagonal H(110) peak intensity.[9] The XRD observations of tetragonal phase recovery are further validated by Raman spectroscopy as shown in Fig. 2(b), where clear

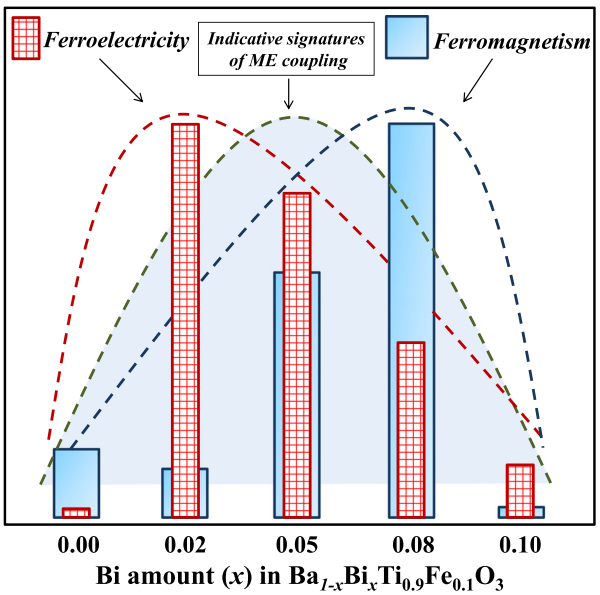

FIG. 1. Schematic representation of the multiferroic response from $Ba_{1-x}Bi_xTi_{0.90}Fe_{0.10}O_3$ compounds. The best ferroelectric and magnetic responses are obtained around $x = 0.02$ and $x = 0.08$ regions, respectively, while the indicative signature of ME coupling becomes the strongest for the intermediate $x = 0.05$ composition (bar height represents the relative strength of the observed physical property).

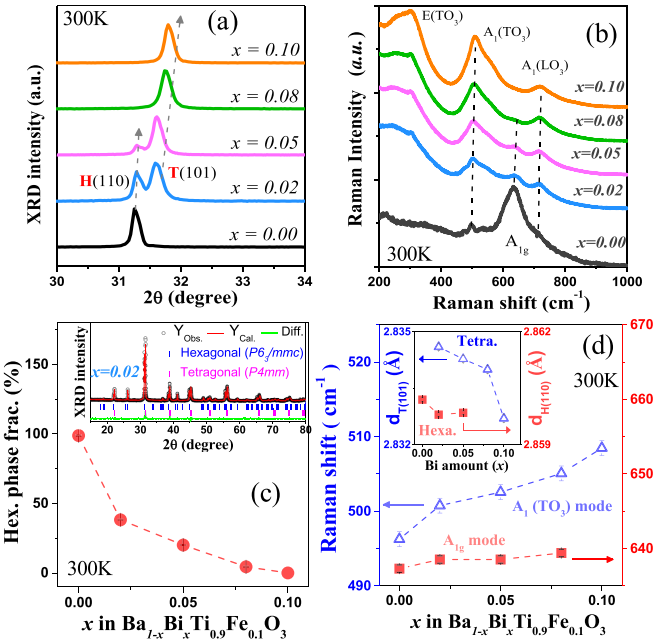

FIG. 2. (a) Room temperature XRD spectra of $Ba_{1-x}Bi_xTi_{0.90}Fe_{0.10}O_3$, (b) corresponding room-temperature Raman spectra, and (c) variation of the hexagonal phase fraction (%). The inset to (c) shows Rietveld refinement for $x = 0.02$ and (d) Raman shifting of the tetragonal $A_1(TO_3)$ mode and hexagonal A_{1g} mode, respectively, while its inset shows the variation of interplannar spacings of hexagonal H(110) and tetragonal T(101) planes, respectively.

evolution of tetragonal Raman modes from the majority hexagonal phase with increasing Bi concentration has been observed.[10,11] The amount of hexagonal [shown in Fig. 2(c)] and tetragonal phase [shown in Fig. 3(b)] fractions present in each of these samples is determined from Rietveld refinement of their room-temperature XRD spectra incorporating both hexagonal ($P6_3/mmc$) and tetragonal ($P4mm$) phases [an example is shown in the inset of Fig. 2(c) for $x = 0.02$, see also Fig. S2 of the supplementary material]. It is interesting to note that there is strong shifting of the tetragonal T(101) XRD peak to higher angles with Bi doping; however, such is not the case for the hexagonal H(110) as shown in Fig. 2(a). Similarly, no significant change in $d_{H(110)}$ [spacing between H(110) planes] is observed beyond $x = 0.02$, whereas $d_{T(101)}$ systematically gets reduced with increasing Bi doping concentration, as shown in the inset to Fig. 2(d). The reduction of $d_{T(101)}$ is driven by the substitution of Ba^{2+} ions by relatively smaller Bi^{3+} ions. Furthermore, we note the monotonic shifting of the tetragonal Raman $A_1(TO_3)$ mode toward higher energy with Bi doping, which is, however, not quite prominent in the case of the hexagonal Raman A_{1g} mode as shown in Fig. 2(d). Thus, both XRD and Raman analyses suggest a maximum doping percentage of Bi at the Ba site of the hexagonal BTO.

Next, to study the intrinsic ferroelectric properties, we have employed the PUND[12,13] technique (for details see Ref. 5). In Fig. 3(a), we see that from $x = 0$ there is a sudden increase in the ferroelectric polarization value for $x = 0.02$ and then it continues to decrease up to $x = 0.10$ (also see Fig. S3 of the supplementary material). However, such a nonmonotonic trend of polarization-change cannot be

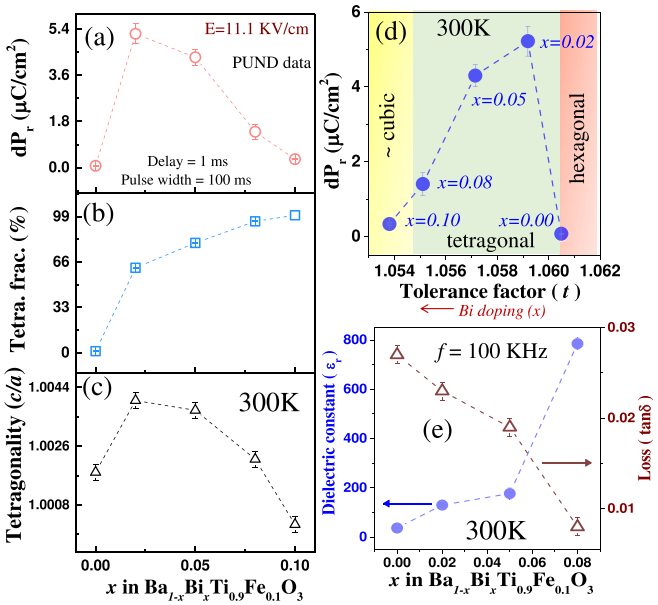

FIG. 3. (a) Variation of remanent-ferroelectric polarization at room temperature, obtained from PUND measurements, (b) and (c) show the variation of tetragonal phase fraction (%) and sample tetragonality (*c*/*a*), respectively. (d) Variation of remanent polarization with the sample tolerance factor, and (e) variation of the dielectric constant and loss tangent values at room temperature with Bi doping amount.

understood from the monotonic evolution of the tetragonal phase fraction (%) as seen in Fig. 3(b). To investigate such a behavior, we have calculated the sample tetragonality (*c*/*a*), which is shown in Fig. 3(c). Here, we note that the tetragonality, which is found to be maximum for $x = 0.02$, exhibits the same trend as observed for polarization change in Fig. 3(a). Therefore, the tetragonality, measure of the amount of Ti-off centric distortion in the corresponding TiO_6 cage[3] (see Fig. S7 of the supplementary material), overrides the amount of tetragonal phase percentage present in regard to the observed ferroelectricity in these systems.[5] Such observations were further validated from temperature dependent pyrocurrent measurements (see Fig. S4 of the supplementary material).

Now, to have a holistic view, we have plotted the remanent polarization value (dPr) vs sample tolerance factor (which can strongly influence structural instabilities of such perovskite oxides[15]) as shown in Fig. 3(d), using Fe and Ti valencies determined from the Fe-K edge XANES and XPS spectroscopic studies[5] (for details see Secs. V–VII of the supplementary material). Interestingly, there is a window of tolerance factor around which ferroelectric response is optimum in these systems, useful for achieving an optimized multiferroic response.

Interestingly, we find a systematic increase in large dielectric constant values as well as reduction in loss tangent values with increasing Bi doping content [see Fig. 3(e)], which makes the higher Bi–Fe codoped system ($x = 0.08$) promising for use as a room-temperature high-κ dielectric material since it exhibits a unique combination of often contradictory physical properties, i.e., very large dielectric constant, extremely low dielectric loss, and moderate temperature dependence of dielectric constant values around room temperature [$TC_\epsilon = (1/\epsilon_r) \times (\partial\epsilon_r/\partial T)$] (see Table I).[14,16] While undoped $BaTiO_3$

TABLE I. Dielectric constant (ϵ_r), dielectric loss (D), and the temperature coefficient of dielectric constant TC_ϵ (which is averaged from 275 K to 325 K temperature window) measured at a frequency of ~100 kHz. Here, only values of SiO_2 and $SrTiO_3$ are taken from previous reports. Reproduced with permission from Choudhury *et al.* Appl. Phys. Lett. **96**, 162903 (2010). Copyright 2010 AIP Publishing.

Sample	Dielectric constant (ϵ_r) 300 K	Loss (D) 300 K	Avg. TC_ϵ (ppm/K) at (300 ± 25) K
SiO_2	3.7	0.0015	…
$SrTiO_3$	285	0.006	−2400
$BaTiO_3$	1626	0.015	−799 ± 408%
$x = 0$	37	0.027	−541 ± 8%
$x = 0.05$	177	0.019	2358 ± 17%
$x = 0.08$	785	0.008	2262 ± 14%

also exhibits a very high dielectric constant and low loss values, but the corresponding $|TC_\epsilon|$ value changes a lot within the 50 K temperature window around room temperature rendering it unsuitable as a high-κ dielectric material. Interestingly, the dielectric response of $x = 0.08$ (i.e., higher dielectric constant value, comparable loss, and $|TC_\epsilon|$ values) seems better compared to $SrTiO_3$, very well-known as a high-κ dielectric material.[17]

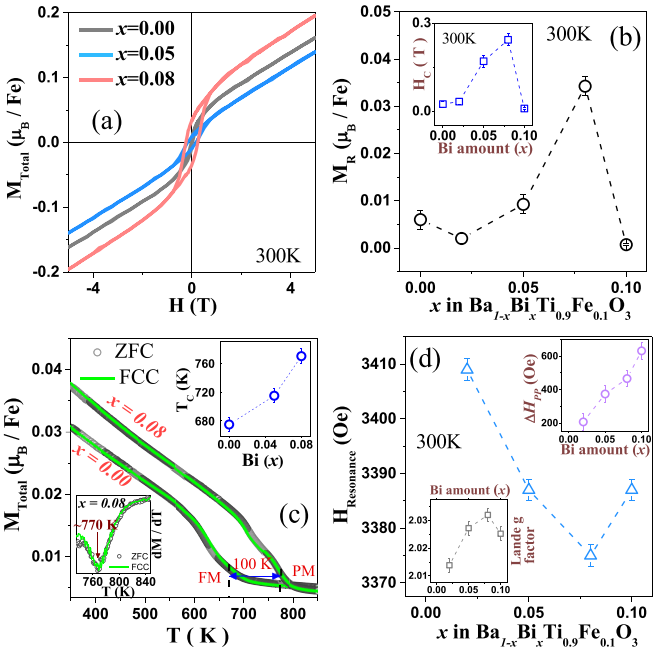

FIG. 4. (a) Room temperature MH plots. (b) Variation of remanent magnetization (M_R). The inset to it shows the corresponding change in coercive field (H_C). (c) Temperature dependent magnetization behavior for applied field of 0.5 T, where bottom and top insets, respectively, show the dM/dT vs T plot and the change in ferromagnetic T_C with Bi doping concentration. (d) and its top inset show variation of resonance magnetic field and H_{PP} (peak to peak linewidth) as determined from EPR spectra, while its bottom inset shows the corresponding change in the Lande g-factor.

To investigate the magnetic properties, first we discuss the room-temperature MH data as shown in Fig. 4(a), which exhibit finite ferromagnetic loops; however, they do not saturate, indicating the presence of some paramagnetic contributions.[18] Thus, we consider the intrinsic ferromagnetic remanent moment (M_R) which is seen to monotonically increase from $x = 0$ up to $x = 0.08$ (having ~6 times enhanced magnetization) and then decreases for $x = 0.10$ as shown in Fig. 4(b). Such a non-monotonic trend is also reflected even in the case of coercive field [see the inset to Fig. 4(b)]. Temperature dependent magnetization measurements display clear ferromagnetic to paramagnetic phase transition and the Curie temperature (T_C) [as estimated from dM/dT vs T plot, shown in the bottom inset to Fig. 4(c)] is found to increase systematically with Bi doping concentration as shown in Fig. 4(c) and its top inset. To further investigate the above trend of magnetization in the microscopic scale, we employ EPR spectroscopy, which is shown in Fig. S10 of the supplementary material, where we see marked changes in line shape with Bi doping. First, we have determined the peak-to-peak linewidth (ΔH_{PP}) [see the top inset of Fig. 4(d)], which increases monotonically with Bi doping, indicating increasing Fe–Fe exchange interaction.[19,20] Subsequently, we see that the resonance magnetic field monotonically decreases up to $x = 0.08$ and then slightly increases for $x = 0.10$. Such observations strongly indicate that the strength of ferromagnetic interaction gets enhanced up to $x = 0.08$, followed by a reduction for $x = 0.10$, possibly due to some antiferromagnetic interaction.[20,21] Even, the Lande g-factor for all these compounds, as shown in the bottom inset of Fig. 4(d), shows a similar trend to the remanent magnetization value. Such enhancement of ferromagnetism, however, cannot be understood from the framework of increasing oxygen vacancy content[19] or increasing hexagonal phase fractions, as both are simultaneously and monotonically reduced with increasing Bi doping concentration.[5] Such trends of magnetic response cannot be understood from the possible presence of any extrinsic contributions, like from $BiFeO_3$, Fe_2O_3, or Fe_3O_4 related impurity phases, which, however, could not be detected through detailed XRD analyses, as discussed in the last section of the supplementary material (also, note Refs. 22–25). These results suggest an alternative source of ferromagnetism for higher x members beyond the hexagonal BTO phase that can likely be the tetragonal BTO phase (Fe^{4+}–O–Fe^{3+}, FM superexchange interaction), as beyond some doping limit both Bi and Fe tend to go into the tetragonal phase (for schematic visualization, see Sec. IX of the supplementary material).

The $x = 0.08$ compound, in addition to possessing ~20 times enhanced ferroelectric remanent polarization value compared to that of $x = 0$ (also, evident from their room-temperature PE loops, shown in Fig. S11 of the supplementary material), is also more insulating than $x = 0$ (the optical bandgap of $x = 0.08$ is greater than that of $x = 0$ as determined from diffused reflectance spectroscopy measurements) as shown in Fig. 5(a). Therefore, $x = 0.08$ (Bi–Fe codoped BTO), which is found to have much enhanced ferroelectric, ferromagnetic, and insulating properties at room-temperature compared to $x = 0$ (only Fe-doped BTO), is more suitable as a better multiferroic. Figure 5(b) and its inset show isothermal MH plots of $x = 0.08$ and $x = 0$, respectively. The difference in 300 K and 10 K MH curves is more prominent in the former than the latter. Variations of their extracted coercive fields (H_C) and remanent magnetizations (M_R) are shown in Fig. 5(c) and its inset. Here, we note that though M_R increases on decreasing temperature like an usual ferromagnet;[26–28]

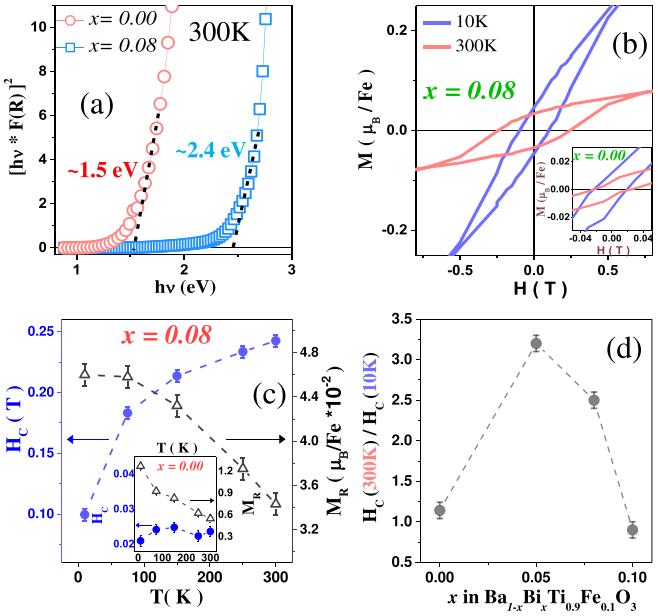

FIG. 5. (a) Kubelka–Munk plots calculated from diffused reflectance spectroscopy, (b) MH plots of $x = 0.08$ at 300 and 10 K, where its inset shows the corresponding MH plots of $x = 0$. (c) and its inset show variations of coercive field (H_C) and remanent magnetization (M_R) with temperature for $x = 0.08$ and $x = 0$, respectively. (d) Variation of the ratio of coercive field (H_C) at 300 and 10 K with Bi doping.

however, the coercive field shows opposite trend. Even, such surprising behavior is stronger in $x = 0.08$ than $x = 0$. It is important to note that such an unusual trend of coercive field with temperature has been used as an indicative (indirect) measure of the ME coupling strength in many related ME multiferroic systems.[29–31] The presence of ME coupling in these compounds also becomes evident from the correlation of the ferroelectric polarization and the spontaneous magnetization at various temperatures, as shown in Fig. S12 of the supplementary material, similar to that observed in the ME multiferroic $0.9BiFeO_3$-$0.1BaTiO_3$ system.[34] Thus, such anomalous temperature dependent variations of magnetic coercivity in our Bi–Fe codoped compounds are likely governed by the competition between magnetocrystalline anisotropy and ME coupling.[31–33] The ratio of H_C at 300 K to H_C at 10 K (the factor of reduction of coercive field) can, thus, be used as an indicative marker for the strength of ME coupling [which is plotted in Fig. 5(d)], which, for this series, becomes the strongest for $x = 0.05$ composition, possibly driven by the right appropriate mix of simultaneously large ferroelectric polarization and ferromagnetic moment value, likely within the same tetragonal phase.

In summary, we have investigated room-temperature multiferroic properties of Ba_{1-x} $Bi_xTi_{0.90}Fe_{0.10}O_3$ ($0 \leq x \leq 0.10$) compounds. By codoping Bi and Fe into $BaTiO_3$, we completely recover the ferroelectric tetragonal phase in the magnetically doped BTO compounds. However, the role of sample tetragonality in the recovered ferroelectricity is found to be stronger. Both macro- and microscopic measurements reveal that the intrinsic ferromagnetic property gets enhanced up to $x = 0.08$ with Bi doping, which is followed up by a reduction for $x = 0.10$ due to increased antiferromagnetic interaction. Interestingly, in this series of compounds, though $x = 0.02$ shows the highest

ferroelectric polarization and $x = 0.08$ shows the largest magnetic moment, however, the signature of ME coupling, as indicated from the anomalous change of magnetic coercive field with temperature, seems to be strongest in the intermediate $x = 0.05$ due to the simultaneous presence of both ferroelectricity and ferromagnetism in significant amounts and likely within the same tetragonal phase. However, it would be interesting to further probe such ME coupling present in these compounds by some direct measurement techniques. Thus, simultaneous Bi–Fe codoped BTO compounds around the compositions $x = 0.05$ to $x = 0.08$ are found to exhibit better room-temperature ME multiferroic properties compared to only Fe doped BTO as shown in Fig. 1.

See the supplementary material for additional supporting data like XRD refinements, XANES, XPS, EPR, and related discussions.

We acknowledge the use of XPS under the DST-FIST (India) facility in the Department of Physics, IIT Kharagpur for this work. P.P. would like to acknowledge the financial support from MHRD, India. D.C. would like to acknowledge SERB, DST, India (Project file no. ECR/2016/000019) and BRNS, DAE (Sanction No. 37(3)/20/23/2016-BRNS) for financial support. D.T. would like to acknowledge financial support by DST under the India@DESY collaboration.

DATA AVAILABILITY

The data that support the findings of this study are available within the article and its supplementary material file.

REFERENCES

[1]N. A. Hill, J. Phys. Chem. B **104**, 6694 (2000).
[2]D. Khomskii, Physics **2**, 20 (2009).
[3]R. E. Cohen, Nature **358**, 136 (1992).
[4]B. Xu, K. B. Yin, J. Lin, Y. D. Xia, X. G. Wan, J. Yin, X. J. Bai, J. Du, and Z. G. Liu, Phys. Rev. B **79**, 134109 (2009).
[5]P. Pal, K. Rudrapal, S. Mahana, S. Yadav, T. Paramanik, S. Mishra, K. Singh, G. Sheet, D. Topwal, A. R. Chaudhuri, and D. Choudhury, Phys. Rev. B **101**, 064409 (2020).
[6]Y. H. Lin, J. Yuan, S. Zhang, Y. Zhang, J. Liu, Y. Wang, and C. W. Nan, Appl. Phys. Lett. **95**, 033105 (2009).
[7]L. B. Luo, Y. G. Zhao, H. F. Tian, J. J. Yang, J. Q. Li, J. J. Ding, B. He, S. Q. Wei, and C. Gao, Phys. Rev. B **79**, 115210 (2009).
[8]N. A. Spaldin and R. Ramesh, Nat. Mater. **18**, 203 (2019).
[9]D. H. Kim and B. W. Lee, J. Korean Phys. Soc. **68**, 574 (2016).
[10]C. H. Perry and D. B. Hall, Phys. Rev. Lett. **15**, 700 (1965).
[11]H. M. Nguyen, N. V. Dang, P. Y. Chuang, T. D. Thanh, C. W. Hu, T. Y. Chen, V. D. Lam, C. H. Lee, and L. V. Hong, Appl. Phys. Lett. **99**, 202501 (2011).
[12]B. Rajeswaran, D. I. Khomskii, A. K. Zvezdin, C. N. R. Rao, and A. Sundaresan, Phys. Rev. B **86**, 214409 (2012).
[13]A. R. Chaudhuri and S. B. Krupanidhi, Solid State Commun. **150**, 660 (2010).
[14]D. Choudhury, A. Venimadhav, C. Kakarla, K. T. Delaney, P. S. Devi, P. Mondal, R. Nirmala, J. Gopalakrishnan, N. A. Spaldin, U. V. Waghmare, and D. D. Sarma, Appl. Phys. Lett. **96**, 162903 (2010).
[15]Z. Li, M. Yang, J. S. Park, S. H. Wei, J. J. Berry, and K. Zhu, Chem. Mater. **28**, 284 (2016).
[16]A. I. Kingon, J. P. Maria, and S. K. Streiffer, Nature **406**, 1032 (2000).
[17]K. Eisenbeiser, J. M. Finder, Z. Yu, J. Ramdani, J. A. Curless, J. A. Hallmark, R. Droopad, W. J. Ooms, L. Salem, S. Bradshaw, and C. D. Overgaard, Appl. Phys. Lett. **76**, 1324 (2000).
[18]D. Karmakar, S. K. Mandal, R. M. Kadam, P. L. Paulose, A. K. Rajarajan, T. K. Nath, A. K. Das, I. Dasgupta, and G. P. Das, Phys. Rev. B **75**, 144404 (2007).
[19]T. Chakraborty, S. Ray, and M. Itoh, Phys. Rev. B **83**, 144407 (2011).
[20]S. D. Bhame, V. L. J. Joly, and P. A. Joy, Phys. Rev. B **72**, 054426 (2005).
[21]J. Gutiérrez, A. Peña, J. M. Barandiarán, J. L. Pizarro, T. Hernández, L. Lezama, M. Insausti, and T. Rojo, Phys. Rev. B **61**, 9028 (2000).
[22]J. Lu, A. Günther, F. Schrettle, F. Mayr, S. Krohns, P. Lunkenheimer, A. Pimenov, V. D. Travkin, A. A. Mukhin, and A. Loidl, Eur. Phys. J. B **75**, 451 (2010).
[23]A. S. Teja and P. Y. Koh, Prog. Cryst. Growth Charact. Mater. **55**, 22 (2009).
[24]Y. Ishikawa and S.-I. Akimoto, J. Phys. Soc. Jpn. **13**, 1298 (1958).
[25]S. Akimoto, T. Katsura, and M. J. Yoshida, J. Geomagn. Geoelectr. **9**, 165 (1957).
[26]X. H. Huang, J. F. Ding, G. Q. Zhang, Y. Hou, Y. P. Yao, and X. G. Li, Phys. Rev. B **78**, 224408 (2008).
[27]V. Markovich, I. Fita, A. Wisniewski, D. Mogilyansky, R. Puzniak, L. Titelman, C. Martin, and G. Gorodetsky, Phys. Rev. B **81**, 094428 (2010).
[28]S. Patankar, S. K. Pandey, V. R. Reddy, A. Gupta, A. Banerjee, and P. Chaddah, Europhys. Lett. **90**, 57007 (2010).
[29]B. Ahmmad, M. Z. Islam, A. Billah, and M. A. Basith, J. Phys. D: Appl. Phys. **49**, 095001 (2016).
[30]T. J. Park, G. C. Papaefthymiou, A. J. Viescas, Y. Lee, H. Zhou, and S. S. Wong, Phys. Rev. B **82**, 024431 (2010).
[31]N. Wang, J. Cheng, A. Pyatakov, A. K. Zvezdin, J. F. Li, D. Viehland, and T. Wu, Phys. Rev. B **72**, 104434 (2005).
[32]R. E. Fayling, J. Appl. Phys. **49**, 1823 (1978).
[33]B. Ruette, S. Zvyagin, A. P. Pyatakov, A. Bush, J. F. Li, V. I. Belotelov, A. K. Zvezdin, and D. Viehland, Phys. Rev. B **69**, 064114 (2004).
[34]A. Singh, V. Pandey, R. K. Kotnala, and D. Pandey, Phys. Rev. Lett. **101**, 247602 (2008).